Chapter 10
Mixer Design for Variability

Both the fabrication process-induced fluctuation and time-dependent degradation cause the MOSFET model parameters to drift. The threshold voltage and mobility are the two most significant model parameters that suffer from process uncertainty and reliability degradations. Here, the most widely used double-balanced Gilbert structure [1] in Fig. 10.1 is used to evaluate the process variations and aging effects on RF mixer performance. In this figure, positive and negative RF input signals are applied to transistors $M1$ and $M2$. Local oscillator (LO) signals are applied to switching transistors $M3$, $M4$, $M5$, and $M6$. The transistor $M7$ provides the bias current. RF and LO multiplication produces the output signal at intermediate frequency (IF).

The conversion gain (CG) of the mixer can be derived as

$$CG = \frac{2}{\pi}\frac{R_L}{R_S + \frac{1}{g_m}} \tag{10.1}$$

where R_L is the load resistance and R_S is the inductor resistance. The noise figure (NF) of the mixer is given by

$$NF = 10\log_{10}(F) \tag{10.2}$$

where F is the flicker noise, which is derived as

$$F = \frac{\pi^2}{4}\left(1 + \frac{2\gamma_1}{g_m R_S} + \frac{2}{g_m^2 R_L R_S}\right) \tag{10.3}$$

and γ_1 is the noise factor.

J.-S. Yuan, *CMOS RF Circuit Design for Reliability and Variability*,
SpringerBriefs in Reliability, DOI 10.1007/978-981-10-0884-9_10

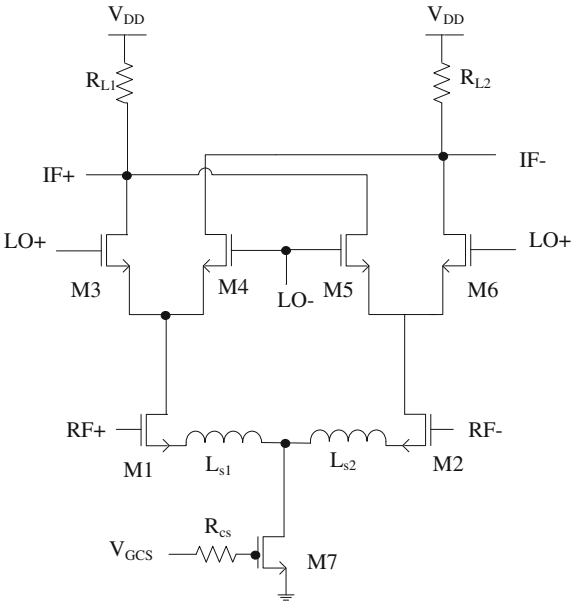

Fig. 10.1 Schematic of a double-balanced Gilbert mixer

The sensitivity of the Gilbert cell mixer can be examined. The process variation and the aging effect may degrade the mixer performance. The conversion gain variation is modeled by the fluctuation of g_m and bias current drift as

$$\Delta CG = \frac{\partial CG}{\partial g_m}\Delta g_m = \frac{\partial CG}{\partial g_m}\left(\frac{\partial g_m}{\partial V_T}\frac{\partial V_T}{\partial I_{\text{bias}}} + \frac{\partial g_m}{\partial \mu_n}\frac{\partial \mu_n}{\partial I_{\text{bias}}}\right)\Delta I_{\text{bias}} \tag{10.4}$$

Expanding the partial derivatives in (10.4) the conversion gain variation can be written as

$$\Delta CG = \frac{2}{\pi g_m^2}\frac{R_L}{(R_S + \frac{1}{g_m})^2} \left\{\frac{I_{\text{bias}}}{(V_{GSM1} - V_T)^2}\frac{L}{\mu_n C_{ox} W_{CS}(V_{GSCS} - V_T)} + \frac{I_{\text{bias}}}{\mu_n (V_{GSM1} - V_T)}\frac{2L}{C_{ox} W_{CS}(V_{GSCS} - V_T)}\right\}\Delta I_{\text{bias}} \tag{10.5}$$

where V_{GSM1} is the gate-source voltage to the RF transistor and V_{GSCS} is the gate-source voltage to the current source transistor.

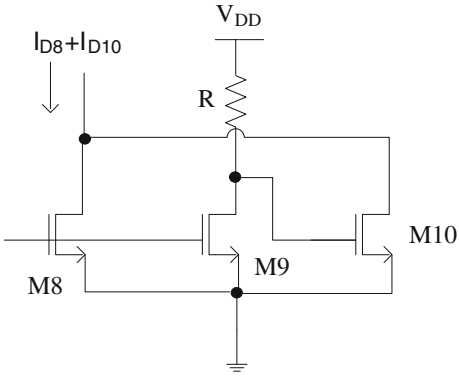

Fig. 10.2 Process insensitive current source

Similarly, the noise figure drift is derived as

$$\begin{aligned}\Delta F &= \frac{\partial F}{\partial g_m}\Delta g_m = \frac{\partial F}{\partial g_m}\left(\frac{\partial g_m}{\partial V_T}\frac{\partial V_T}{\partial I_{\text{bias}}} + \frac{\partial g_m}{\partial \mu_n}\frac{\partial \mu_n}{\partial I_{\text{bias}}}\right)\Delta I_{\text{bias}} \\ &= \left\{\frac{\pi^2}{4}\left(\frac{-2\gamma}{g_m^2 R_S} - \frac{1}{g_m^3 R_L R_S}\right)\right\} \\ &\quad \left\{\frac{I_{\text{bias}}}{(V_{GSM}-V_T)^2}\frac{L}{\mu_n C_{ox} W_{CS}(V_{GSCS}-V_T)} + \frac{I_{\text{bias}}}{\mu_n(V_{GSM}-V_T)}\frac{2L}{C_{ox}W_{CS}(V_{GSCS}-V_T)}\right\}\Delta I_{\text{bias}}\end{aligned} \tag{10.6}$$

Equations (10.5) and (10.6) account for process variations and aging effect of the mixer.

It is clear from (10.4) to (10.6) that the mixer performance is dependent on the drain current of current source. To maintain the mixer performance, the drain current of *M*7 has to be kept stable. Thus, the process invariant current source circuit shown in Fig. 10.2 is employed. In Fig. 10.2, drain currents of *M*8 and *M*9 are designed the same. Changes in *M*8 and *M*10 drain currents are negatively correlated to remain as a stable bias current ($I_{D8} + I_{D10}$). For example, if the process variation increases the threshold voltage, which decreases the drain current of *M*8, the gate voltage of *M*10 increases ($V_{G10} = V_{DD} - I_{D9}R$). Thus, the drain current of *M*10 increases to compensate the loss of I_{D8}.

ADS simulation is used to compare the mixer performance using the single transistor current source versus process invariant current source [2]. The RF mixer is operated at 900 MHz with an intermediate frequency of 200 MHz. In the circuit design, CMOS 0.18 μm mixed-signal technology node is used. R_{L1} is 210 Ω and R_{L2} is 190 Ω. The transistor channel width of *M*3–*M*6 is 200 μm. The channel widths of *M*1 and M2 are 190 and 210 μm, respectively. L_{s1} and L_{s2} are chosen at 2 nH. The width of *M*7 is 250 μm. The gate resistor size of the current source is 400 Ω. The mixer sets the gate biasing voltage at the current source at 0.62 V. In the current source, the transistor *M*8 and *M*9 match each other as 100 μm. The width of *M*10 is 600 μm. The supply voltage V_{DD} is 1.8 V.

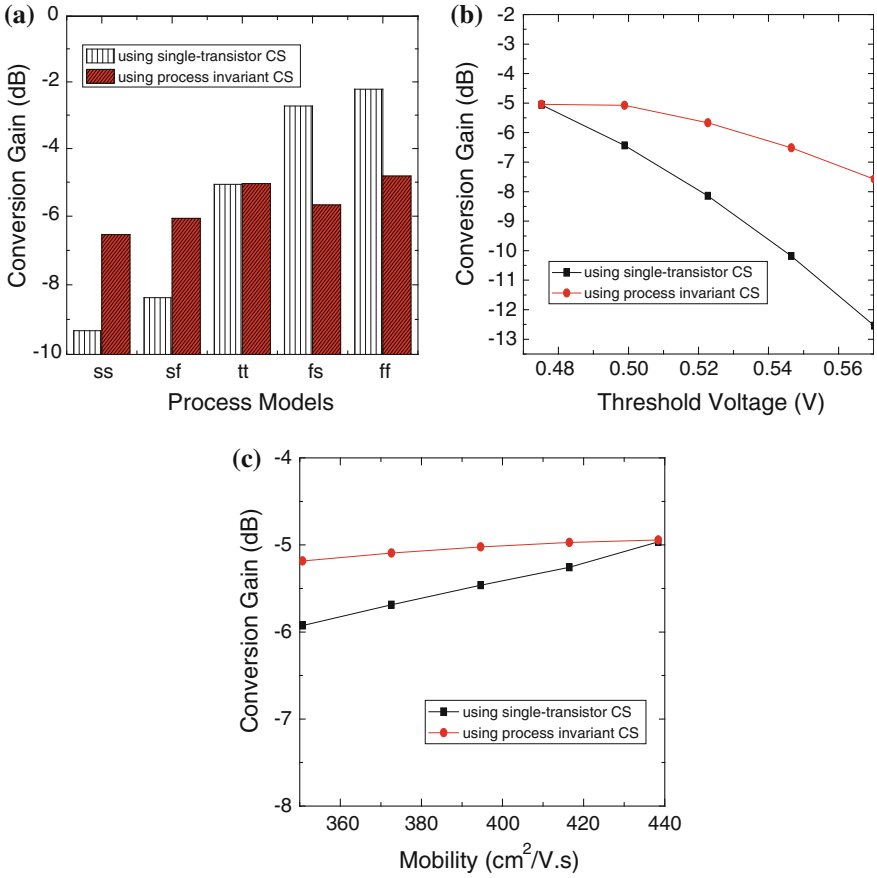

Fig. 10.3 **a** Conversion gain predicted by different process models. **b** Conversion gain versus threshold voltage. **c** Conversion gain versus electron mobility

For the process variation effect, the conversion gain of the mixer is evaluated using different process corner models due to inter-die variations. The simulation result of the fast-fast, slow-slow, slow-fast, fast-slow, and normal-normal models is shown in Fig. 10.3a. It is clear from Fig. 10.3a that the mixer with the invariant current source shows robust conversion gain against different process variations.

The conversion gain is also evaluated using different threshold voltage and mobility degradations resulting from aging (hot carrier effect) as shown in Fig. 10.3b, c. The hot carrier injection increases the threshold voltage, but decreases the electron mobility. The conversion gain decreases with an increased threshold voltage or decreased mobility due to reduced transconductance. Again, the mixer with process invariant current source exhibits more robust performance against threshold voltage increase and mobility degradation.

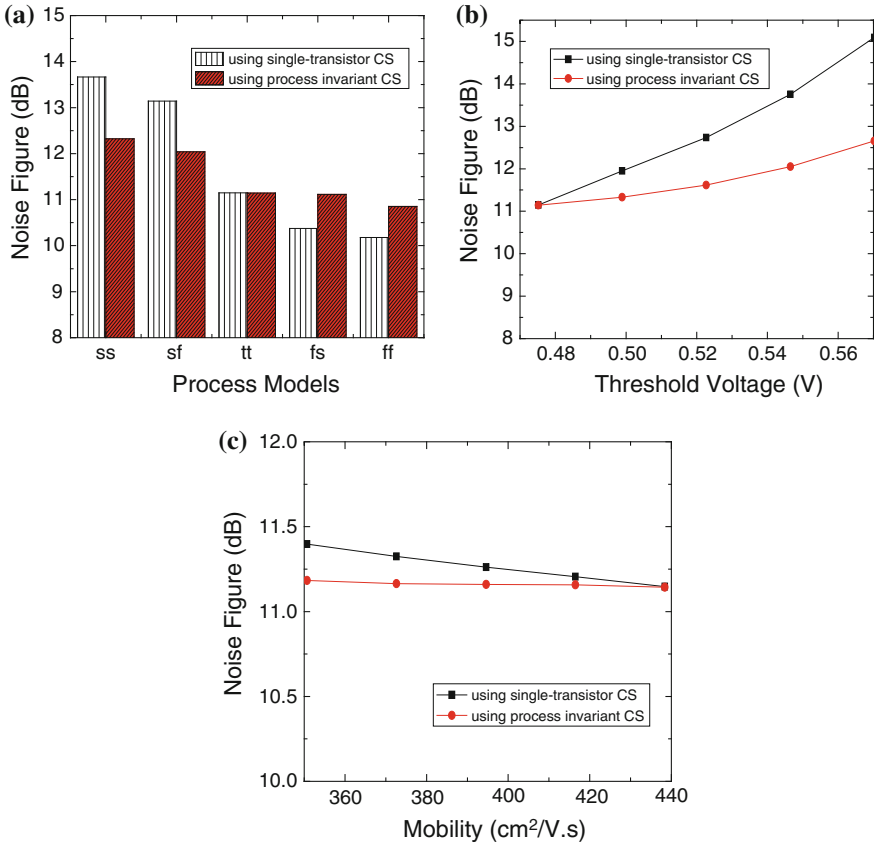

Fig. 10.4 **a** Noise figure predicted using different process models. **b** Noise figure versus threshold voltage. **c** Noise figure versus electron mobility

In addition, the noise figure of the mixer using the process invariant current source is compared with that using the single transistor current source. The noise figure versus different process models is displayed in Fig. 10.4a. It is clear from Fig. 10.4a that the noise figure is more stable over different corner models for the mixer using the current invariant current source. The noise figure also shows less threshold voltage and mobility sensitivity as evidenced in Fig. 10.4b, c. In Figs. 10.4b and 10.5c, the noise figure increases with increased threshold voltage and decreased mobility due to reduced drain current and transconductance in the mixer.

The output power of the mixer has been evaluated using different process corner models as well. As shown in Fig. 10.5a the output power of the mixer using the process invariant current source demonstrates robust performance against process variations. In Fig. 10.5b, c the output power decreases with increased threshold voltage and decreased mobility due to reduced drain current in the mixer. The

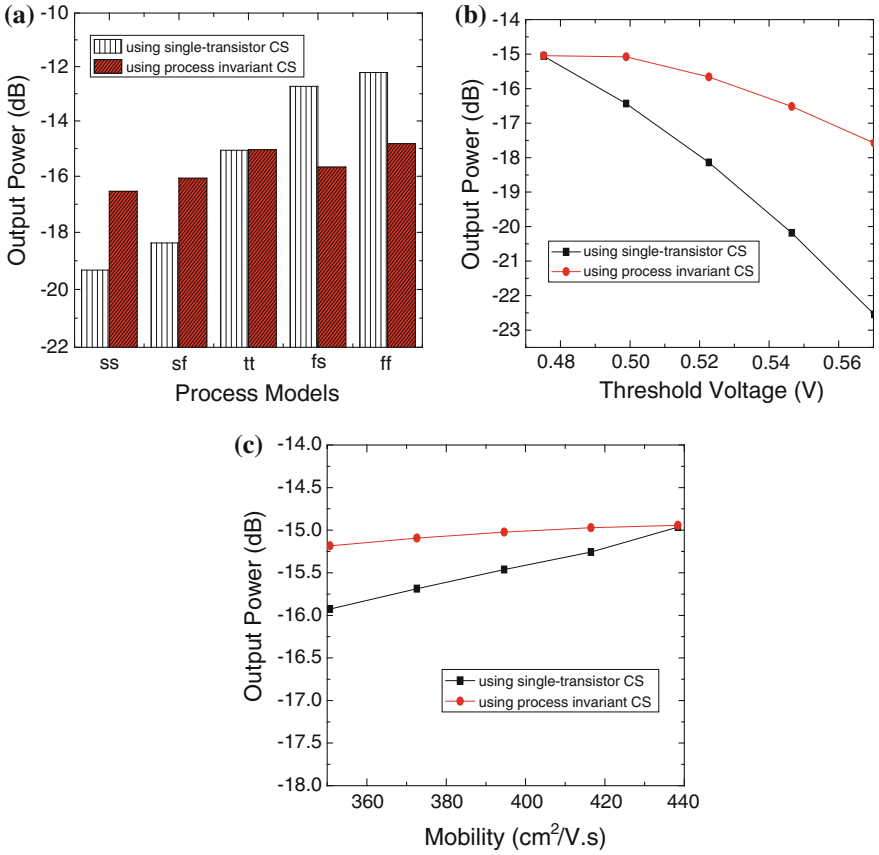

Fig. 10.5 **a** Predicted mixer out power using different process models. **b** Output power versus threshold voltage. **c** Output versus electron mobility

output power in Fig. 10.5b, c also shows less sensitivity against aging effect, which increases the threshold voltage and decreases the electron mobility.

The output power of the mixer has been evaluated using different process corner models as well. As shown in Fig. 10.5a the output power of the mixer using the process invariant current source demonstrates robust performance against process variations. In Fig. 10.5b, c the output power decreases with increased threshold voltage and decreased mobility due to reduced drain current in the mixer. The output power in Fig. 10.5b, c also shows less sensitivity against aging effect which increases the threshold voltage and decreases the electron mobility.

To further examine the process variation and reliability impact on RF mixer, Monte Carlo (MC) circuit simulation has been performed. In ADS, the Monte Carlo simulation [3] assumes statistical variations (Gaussian distribution) of transistor model parameters such as the threshold voltage, mobility, and oxide thickness. In the Monte Carlo simulation, a sample size of 1000 runs is adopted. Figure 10.6a, b

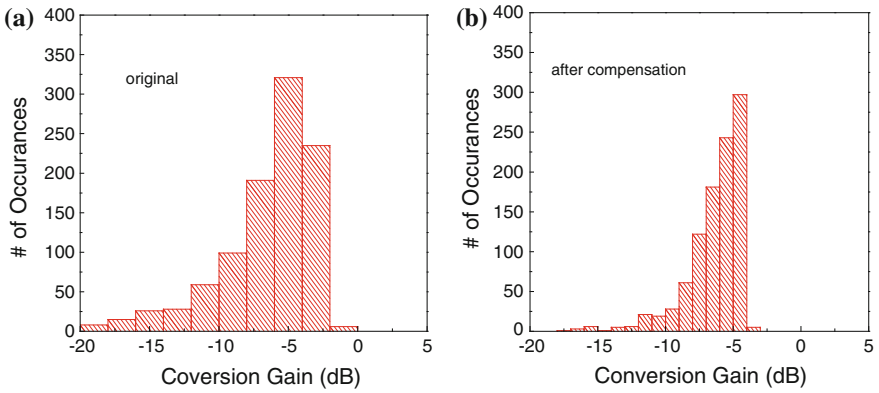

Fig. 10.6 **a** Conversion gain statistical distribution without compensation. **b** Conversion gain statistical distribution after process compensation effect

display the histograms of conversion gain using single transistor current source (original) and using the process invariant current source (after compensation). For the mixer using the traditional current source, the mean value of conversion gain is −6.608 dB and its standard deviation is 3.18 %. When the process invariant current source is used, the mean value of conversion gain changes to −6.324 dB and its standard deviation reduces to 2.08 %.

The noise figure after 1000 runs of Monte Carlo simulation is dialyzed in Fig. 10.7a, b. For the mixer using the single transistor current source, the mean value of noise figure is 11.667 dB and its standard deviation is 2.49 %. When the process invariant current source is adopted, the mean value of noise figure changes to 11.159 dB and its standard deviation reduces to 1.29 %. Clearly, the mixer using

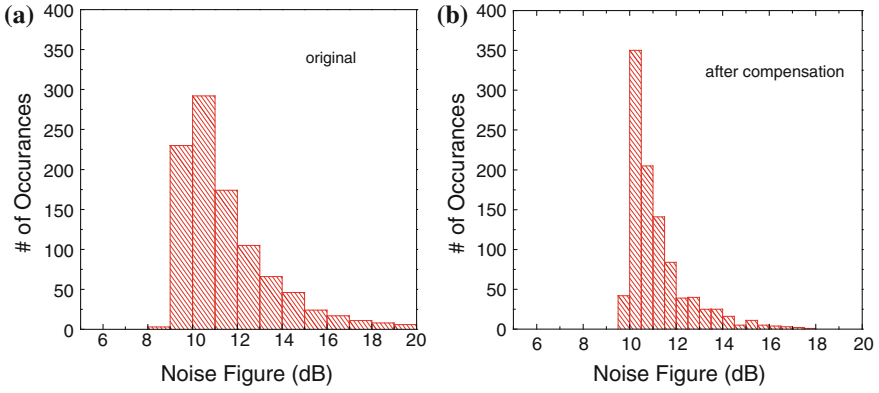

Fig. 10.7 **a** Noise figure statistical distribution without current compensation. **b** Noise figure statistical distribution after process compensation effect

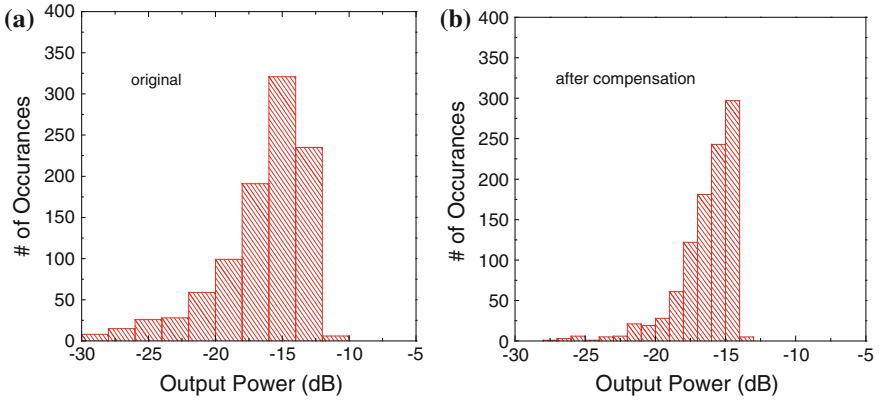

Fig. 10.8 **a** Output power statistical distribution without current compensation. **b** Output power statistical distribution after process compensation effect

the process invariant current source shows better stability against statistics process variations.

In addition, the output power of the mixer is examined in Monte Carlo simulation. Figure 10.8a, b demonstrates an improvement of output power for the mixer using the process invariant current source over that using the traditional current source. In Fig. 10.8, the mean value of output power changes from −16.608 to −16.324 dB and its standard derivation reduces from 3.81 to 2.08 % once the process invariant current source is used.

References

1. Lee TH (1998) The design of CMOS radio-frequency integrated circuits. Cambridge University Press
2. Pappu AM, Zhang X, Harrison AV, Apsel AB (2007) Process invariant current source design: methodology and examples. IEEE J Solid-State Circuits 2293–2302
3. http://www.agilent.com/find/eesof-ads